ELSEVIER

Nuclear Instruments and Methods in Physics Research A 482 (2002) 537–546

NUCLEAR INSTRUMENTS & METHODS IN PHYSICS RESEARCH Section A

www.elsevier.com/locate/nima

Monte Carlo studies of accelerator driven systems: energy and spatial distribution of neutrons in multiplying and non-multiplying media

S.R. Hashemi-Nezhad[a,*], R. Brandt[b], W. Westmeier[b,1], V.P. Bamblevski[c], M.I. Krivopustov[c], B.A. Kulakov[c], A.N. Sosnin[c], J.-S. Wan[d], R. Odoj[e]

[a] *Department of High Energy Physics, School of Physics, A28, University of Sydney, Sydney, NSW 2006, Australia*
[b] *Institut für Physikalische, Kern- und Makromolekulare Chemie, FB 15, Philipps-Universität, Marburg, Germany*
[c] *Joint Institute for Nuclear Research, JINR, Dubna, Russia*
[d] *Northwest Institute of Nuclear Technology, 710024 Xian, China*
[e] *Institut fuer Sicherheitsforschung und Reaktorsicherheit, Forschungszentrum Juelich GmbH, Juelich, Germany*

Received 2 October 2000; received in revised form 7 May 2001; accepted 2 July 2001

Abstract

The LAHET code system is used to study the behaviour of the spallation neutrons resulting from the interaction of 2.5 GeV/c protons with a massive lead target within a large ($\sim 32\,m^3$) lead and graphite moderating environments. The spatial and energy distribution of the neutrons with presence and absence of a fissile material in Accelerator Driven Systems (ADS) are investigated.

It is shown that the energy spectra of the neutrons in graphite and lead moderators are very different and such difference is expected to result in noticeable differences in the nuclear waste transmutation abilities of the ADSs that use graphite and lead for neutron moderation and storage.

PACS: 28.20; 28.20G; 28.41; 28.50

Keywords: Accelerator-driven systems; Spallation neutrons; Energy amplifier; Nuclear waste transmutation

1. Introduction

Neutrons produced in the interaction of relativistic projectiles with heavy targets (e.g. protons on lead) can be used for energy production and nuclear waste transmutation, in Sub-critical Nuclear Assemblies (SNA), [1–3]. These systems are also known as Accelerator Driven Systems (ADS).

It is suggested that an effective method for nuclear waste transmutation is to use neutron capture in the resonance region of the absorption cross-section of the waste isotopes. This method is known as transmutation by adiabatic resonance

*Corresponding author. Tel.: +61-2-9351-5964; fax: +61-2-9351-7727.

E-mail address: reza@physics.usyd.edu.au (S.R. Hashemi-Nezhad).

[1] Permanent address: Dr. Westmeier GmbH, 35085 Ebsdorfergrund, Germany.

0168-9002/02/$ - see front matter
PII: S0168-9002(01)01507-8

crossing (TARC), when a heavy (e.g. Pb) moderating environment is used [4,5].

As the effectiveness of TARC is highly dependent on the flux and energy distribution of the neutrons at the waste sample location, it is important to investigate how neutron energy distribution and flux varies with distance from the centre of the cascade.

In a realistic ADS, there will be fissile materials in the system [2,6,7]. Such fissile materials are present either as fuel *only* (e.g. ^{233}U, ^{235}U) or as combined fuel-waste, such as Pu isotopes. Therefore, we studied ADSs that contained a fissile material in the system.

2. Calculation procedure

The behaviour of the spallation neutrons produced in the interaction of high-energy protons with thick lead target embedded within a large moderating environment was studied. The spatial distribution of the neutron flux and the neutron energy distribution in the moderator with and without the presence of a neutron-multiplying medium, was calculated using the LAHET code system [8]. The neutron multiplying region refers to the one that contains fissile materials. In the present paper three different cases will be considered (see Fig. 1): (a) lead target and lead moderator without presence of neutron-multiplying medium, (Pb, Pb, 0) system; (b) lead target, lead moderator plus a ^{235}U neutron multiplying region, (Pb, Pb, ^{235}U) system; and (c) lead target and graphite moderator without a neutron multiplying region, (Pb, C, 0) system.

Fig. 1 shows the XZ-cross-section of the all components of the three assemblies used in the calculations. In all of the above-mentioned cases, the moderator occupied a volume of $3.3 \times 3.3 \times 3\,\mathrm{m}^3$ ($\sim 32\,\mathrm{m}^3$) and target and multiplying region (if present) were embedded in the moderator. In the case of the (Pb, Pb, 0) and (Pb, Pb,^{235}U) systems the whole ~ 370 tons of lead acts as target and moderator. While in the (Pb, C, 0) system a cylindrical lead target of diameter 20 cm and length of 1 m was placed on the Z-axis starting from $Z = -30$ cm.

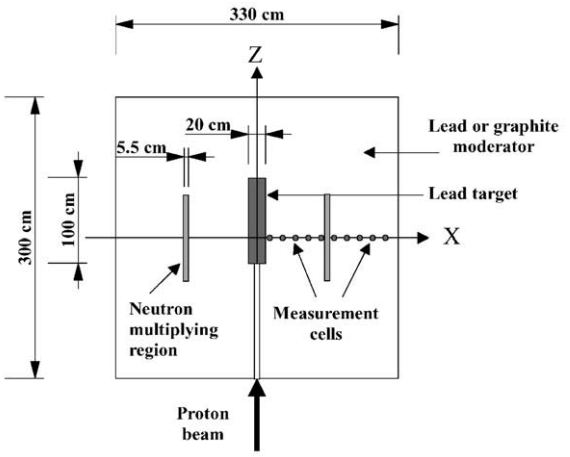

Fig. 1. XZ-cross-section of the target-moderator-multiplier assemblies used in the LAHET Monte Carlo simulations. The origin of the Cartesian co-ordinate system corresponds to the centre of the assembly. Note that not all of the components shown in figure were present in every simulation. (For dimensions and details of the set-ups refer to the text.).

To model the effects of a neutron-multiplying medium on the neutron flux and energy distribution, a cylindrical stainless steel shell container filled with UO_2, was placed within the lead assembly. The axis of fuel container and beam axis is concentric and its centre coincides with the centre of the assembly (Fig. 1). The wall thickness of the container was 2 mm and it had inner and outer diameters of 79.8 and 85.2 cm respectively. The length of the fuel container was 100 cm. It was assumed that 20% of the U-atoms in UO_2 are ^{235}U. In the design of the target-moderator-multiplier systems, technical considerations are not taken into account. In particular, the chemical composition of the fissile material in the multiplying region is chosen arbitrarily.

In all target-moderator assemblies ten spheres of radius 3 cm filled with the corresponding moderator medium were located on the X-axis starting from $x = 15$ cm at intervals of 15 cm which were used as measurement (calculation) cells (Fig. 1). In the case of the (Pb, Pb, 0) seven extra spherical cells of diameter 1 cm were located at $x < 15$ cm with intervals of 2 cm, starting from $x = 0$ cm, (these are not shown in Fig. 1).

Protons of momentum 2.5 GeV/c (kinetic energy $E_p = 1732$ MeV) were used in all calculations. The protons were introduced into the system along the Z-axis through a 1.2 m long blind hole of diameter 6 cm. The proton beam had circular cross-section with a diameter of 1 cm.

The LAHET code [8], which is coupled with the MCNP code [9] deals with spallation processes involving hadronic interactions and transports the produced neutrons (in our case) down to 20 MeV. Neutrons of energy less than 20 MeV are transported with MCNP code, which in our case was version MCNP-4B2. In LAHET calculations we used the following input options: (1) Bertini model of intranuclear cascade; (2) pre-equilibrium model following the intranuclear cascade; (3) Gilbert–Cameron–Cook–Ignatyuk level density model; (4) Coulomb barrier on incident charged particle interactions; and (5) Rutherford–Appleton Laboratory evaporation-fission model. In this paper the term "spallation neutrons" refers to neutrons produced by high-energy proton reactions in the intranuclear cascade, evaporation and high-energy fission processes as well as those produced in inter-nuclear-cascade.

For every calculation 25,000–50,000 incident proton histories were followed and results were normalized to 10^9 protons per second, corresponding to a beam current of $I = 0.16$ nA.

3. Results and discussion

3.1. Energy spectrum of spallation nucleons

Fig. 2 shows the energy distribution of the nucleons resulting from the spallation process when protons of energy 1.73 GeV impinge on Pb-targets of (Pb, Pb, 0) and (Pb, C, 0) systems. The difference between the spallation nucleon energy distributions in the two systems may be summarised as follows:

1. The energy distribution of the spallation neutrons in two target-moderator assemblies of (Pb, C, 0) and (Pb, Pb, 0) are rather similar.

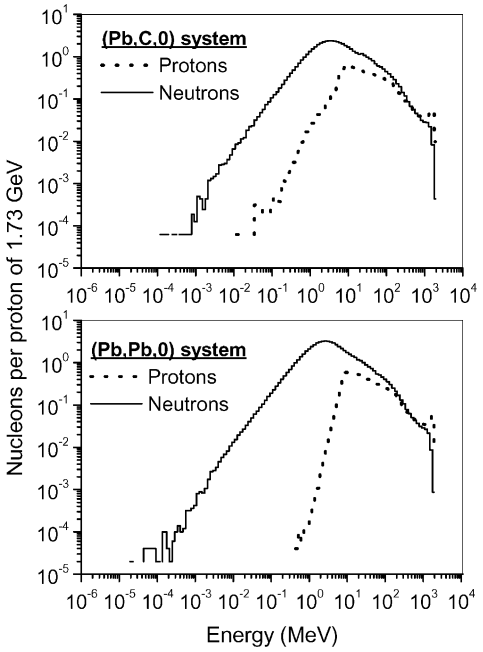

Fig. 2. Energy distribution of the nucleons resulting from the spallation process when protons of energy 1.73 GeV impinge on Pb-targets of (Pb, Pb, 0) and (Pb, C, 0) systems.

2. The peaks of the neutron distributions appear at energy interval of 2.7–3.7 MeV in both systems.
3. The energy distribution of the spallation protons in the two systems are different and the distribution in (Pb, C, 0) extends to lower-energy than (Pb, Pb, 0) system.
4. The peak of the proton distributions appear at energies of 8.5 and 10 MeV for (Pb, C, 0) and (Pb, Pb, 0) systems, respectively.

Table 1 gives the total number of spallation neutrons, Y_n produced in each of the ADS studied. Also given is the number of neutrons that leak out of each system per incident proton, Y_l. The last column of the Table 1 gives the fraction of the total number of neutrons that leak out of the system. In the case of the (Pb, Pb, ^{235}U) system, leakage neutrons include the neutrons that are produced in the neutron multiplying region via fission. The cylindrical neutron multiplying shell in (Pb, Pb, ^{235}U) contains 2.77 tons of UO_2 from

Table 1
Spallation neutron yield and neutron leakage from the system per incident proton of $E_p = 1.73$ GeV

Type of ADS	Spallation neutron yield Y_n	Neutron leakage from system	
		Leakage Y_l	Percentage of total neutrons in system
(Pb, Pb,0)	66.23 ± 0.07	21.71 ± 0.03	32.8 ± 0.06
(Pb, C,0)	52.38 ± 0.16	7.20 ± 0.02	13.7 ± 0.06
(Pb, Pb,^{235}U)	66.11 ± 0.07	90.29 ± 0.69	15.0 ± 1.1

which 488.3 kg is ^{235}U. For this system an effective neutron multiplication coefficient of $k_{eff} = 0.8891 \pm 0.0005$ was calculated using MCNP-4B2 code [9]. In (Pb, Pb, ^{235}U) the $Y_n = 66.11$ spallation neutrons multiply to $N_t = 596$ neutrons. Neutron leakage from the (Pb, Pb, ^{235}U) system is $\sim 50\%$ of that from the (Pb, Pb, 0) system. This is due to the fact that in (Pb, Pb, ^{235}U) the majority of the neutrons have fission origin and so have different energy distribution compared to that of the spallation neutrons. The difference $Y_a = N_t - Y_l$ is the number of the neutrons per incident proton, that are absorbed in each system (for non-multiplying systems $N_t = Y_n$). Although because of difference in target size number of spallation neutrons in (Pb, Pb, 0) and (Pb, C, 0) systems are different [10], but the number of the absorbed neutrons in two systems are about the same ($Y_a = 45$).

3.2. Energy spectrum of neutrons in the moderator

3.2.1. (Pb, Pb, 0) system

Fig. 3a shows the neutron flux ($E \times dF/dE$) as a function of energy for the (Pb, Pb, 0) system, at different positions on the X-axis. From Fig. 3a it can be seen that;

- In a large lead moderator and in the absence of a neutron-multiplying medium, even in the vicinity of the beam line the neutron flux at given x-value does not vary substantially with increasing energy in the energy range of 1 eV–1 MeV. Within this energy range there is a factor of < 70 increase in the neutron flux for a 6 orders of magnitude increase in the energy. For neutrons in the energy interval of 1 eV–1 keV this factor is only ~ 4.
- The maximum of the energy distributions appears at $E \approx 520$ keV independent of the location in the moderator. Due to slowing down of neutrons, the width of this peak increases with increasing x and becomes less pronounced, to the extent that neutron flux becomes almost constant in the energy interval of 1 eV–100 keV.
- It is quite interesting to note that the variation of the neutron flux with energy at $x = 0$ (i.e. a location within the target and on the beam line) and $x = 15$ cm in the energy interval 1 eV–~ 100 keV are almost the same.

3.2.2. (Pb,Pb,^{235}U) system

Fig. 3b illustrates the neutron flux ($E \times dF/dE$) as a function of energy for (Pb,Pb,^{235}U) system.

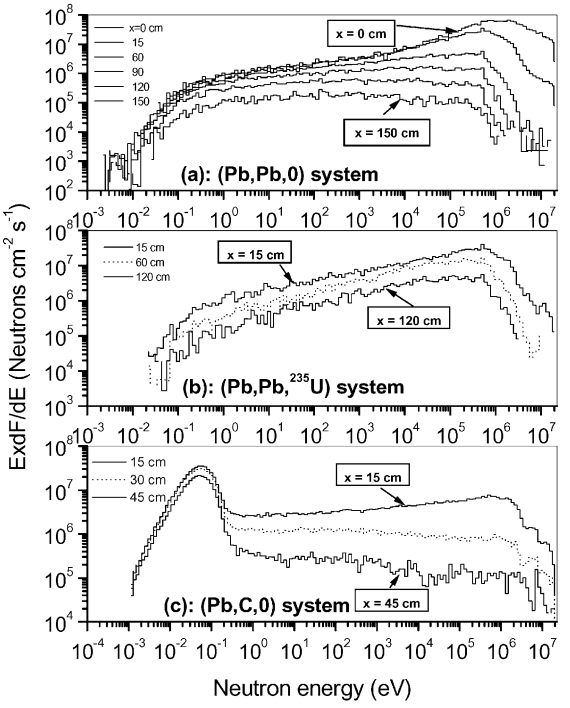

Fig. 3. Neutron flux $E \times dF/dE$ as a function of energy (a) (Pb, Pb, 0), (b) (Pb, Pb, ^{235}U) and (c) (Pb,C,0) system at different locations in the moderator (see the text for details).

A comparison of the Figs. 3a and b shows that, qualitatively, the presence of a multiplying medium and addition of fission neutrons to the system has not altered the overall shape of the energy distributions of the neutrons significantly, in the vicinity of the centre. However in the regions close to the multiplying region e.g. $x = 75-90$ cm and also in areas far away from this region e.g. $x \geqslant 120$ cm the energy distributions of the neutrons are significantly different from those in the (Pb, Pb, 0) system at the corresponding locations. For example at $x = 120$ cm for (Pb, Pb, 0) system the neutron flux in the energy range of 1 eV–100 keV remains *almost* constant, while for the case of (Pb, Pb,^{235}U) there is more than an order of magnitude flux increase for the same energy interval. Despite the addition of fission neutrons to spallation neutrons, the peak of the energy distribution appears at ~ 520 keV, the same as for the (Pb, Pb, 0) system.

3.2.3. (Pb,C,0) system

Fig. 3c illustrates the variation of the neutron flux with energy for (Pb,C,0) system in the neighbourhood of the target, at three different locations on the X-axis. Due to very rapid thermalisation of the neutrons in graphite moderator, the flux of the high-energy neutrons drops dramatically and statistical error in high-energy bins becomes increasingly larger with increasing distance from the centre of the assembly. The shape of the energy distributions for (Pb, C, 0) are very different compared to the case for lead moderator. As expected the slow neutrons constitute a large fraction of the total neutron flux $F(x)$, in a given location in the moderator. Fig. 4 shows $\mathrm{R} = F(x)_{(E_n \leqslant 1\ \mathrm{eV})}/F(x)_{(E_n \leqslant 20\ \mathrm{MeV})}$, the ratio of the slow neutron flux ($E_n \leqslant 1$ eV) to flux of neutrons with $E_n \leqslant 20$ MeV, as a function of distance x, for the (Pb, C, 0) and (Pb, Pb, 0) systems. For lead moderator, at most 8.4% of the total neutrons are slow ($E_n \leqslant 1$ eV), see Ref. [11] for more details. This occurs in cell 10 ($x = 150$ cm) where the overall neutron flux is quite low. In the case of the graphite moderator for $x \geqslant 60$ cm almost all neutrons are slow. For (Pb, C, 0) at higher energies (1 eV–1 MeV) the variation of the neutron flux with energy is not substantial (Fig. 3c). This is especially true for $x < 50$ cm.

3.3. General discussion of the energy spectra

For large structures of heavy moderators such as graphite and lead with $\Sigma_a \ll \Sigma_s$, the conditions for applicability of Fermi Age Theory are well fulfilled (Σ_a and Σ_s are macroscopic absorption and scattering cross-sections, respectively).

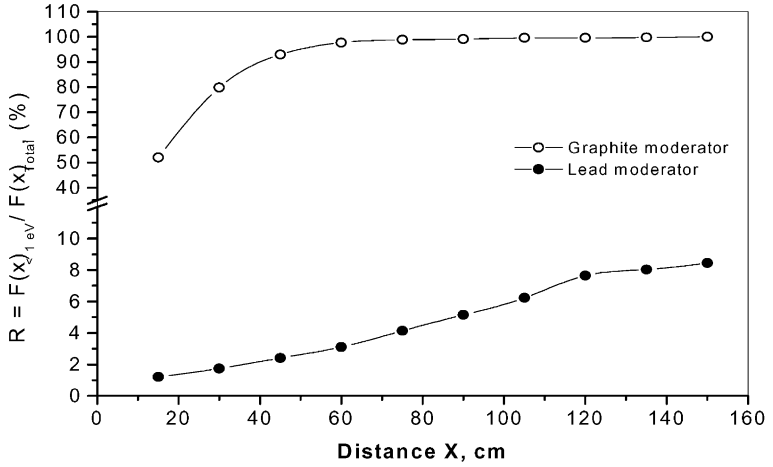

Fig. 4. Variation of the $\mathrm{R} = F(x)_{(E_n \leqslant 1\ \mathrm{eV})}/F(x)_{(E_n \leqslant 20\ \mathrm{MeV})}$ ratio of slow neutron flux ($E_n \leqslant 1$ eV) to total neutron flux ($E_n \leqslant 20$ MeV) as a function of distance x, for the (Pb, C, 0) and (Pb, Pb, 0) systems.

Therefore one expects that the total number neutrons in the system slowing down above any given lethargy, to be independent of lethargy (see e.g. Ref. [12]).

From Fig. 3 it can be seen that in the energy interval of 1 eV–$\sim$1 MeV the above-mentioned expectation is relatively well achieved and there is very little change in the neutron flux in this very wide range of energy (or lethargy). The thermal Maxwellian maximum only is present when there is a weak absorption during moderation i.e. $\Sigma_a(kT_0) << \xi\Sigma_s$ (i.e. moderation ratio much greater than unity), where kT_0 is the thermal energy and ξ is average logarithmic energy loss. This condition is very well satisfied for graphite but not for the lead moderator

$$\Sigma_a(kT_0) = 0.006\,\xi\Sigma_s\,\mathrm{cm}^{-1} \quad \text{(for graphite)}$$

$$\Sigma_a(kT_0) = 1.605\,\xi\Sigma_s\,\mathrm{cm}^{-1} \quad \text{(for lead).}$$

4. Spatial distribution of neutrons

Fig. 5 shows the variation of the flux, for neutrons of $E_n \leqslant 20$ MeV with the distance x on the X-axis ($x \geqslant 15$ cm), for all three systems studied. For target-moderator assemblies in the *absence* of a multiplying medium, neutron flux as a function of distance from the centre, can be described very well with an exponential attenuation curve of the form

$$F(x) = y_0 + Ae^{-(x-x_0)/t}, \quad x \geqslant 15\,\mathrm{cm}. \tag{1}$$

The fitting parameters for 10^9 incident protons are given in Table 2. Note that the number of the primary neutrons produced in the (Pb, Pb, 0) and (Pb, C, 0) is not the same (Table 1). The "attenuation length" t, of the neutrons in two systems are different and neutron number in the (Pb, C,0) attenuate faster. For these two cases

Table 2
Fitting parameters of Eq. (1) for the variation of the neutron flux $F(x)$ as a function of x for neutrons of $E_n \leqslant 20$ MeV. Parameters x_0, t and $L_{1/2}$ are in units of cm

(Pb, Pb, 0)[a]	(Pb, C, 0)[b]
$y_0 = 0 \pm 0$	$y_0 = 0 \pm 0$
$x_0 = 15 \pm 0$	$x_0 = 15 \pm 0$
$A = (731.327 \pm 7.578) \times 10^6$	$A = (825.991 \pm 7.662) \times 10^6$
$t = 36.086 \pm 0.647$	$t = 26.717 \pm 0.454$
$L_{1/2} = 25.013 \pm 0.448$	$L_{1/2} = 18.519 \pm 0.315$

[a](Pb, Pb, 0)–Pb-target, Pb-moderator without neutron multiplier.

[b](Pb, C, 0)–Pb-target, graphite-moderator without neutron multiplier.

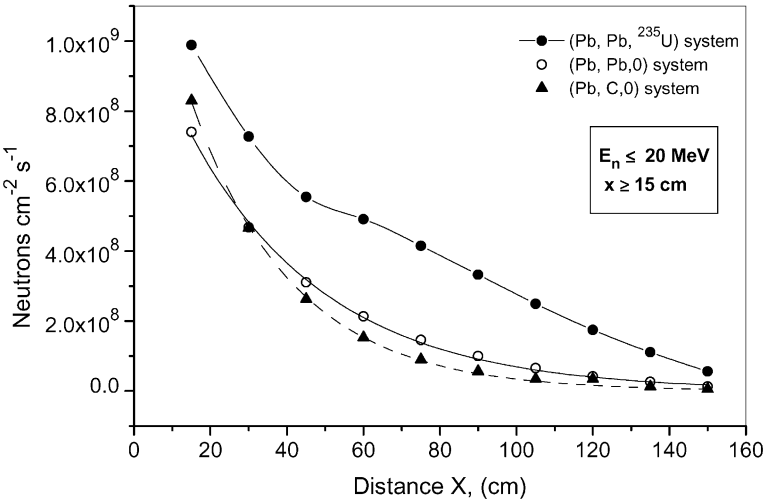

Fig. 5. Variation of flux of neutrons of energy $\leqslant 20$ MeV with distance from the centre of the assemblies. Distance x, was measured on the X-axis (see Fig. 1).

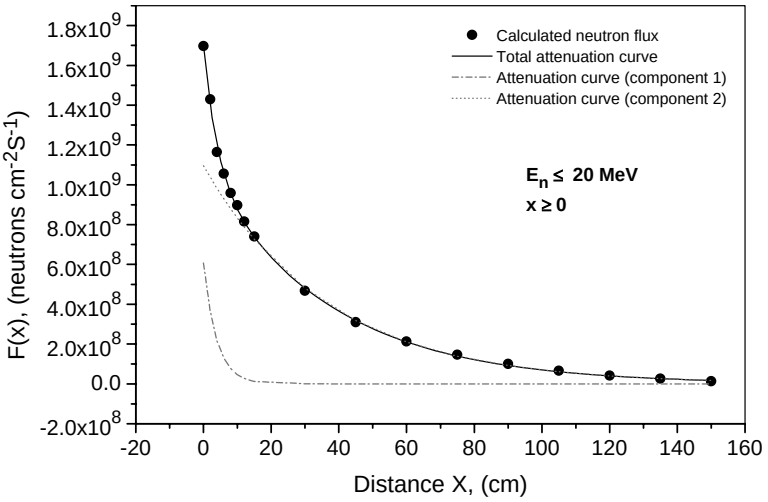

Fig. 6. Flux of neutrons of $E_n \leqslant 20$ MeV as a function of distance x (on the X-axis, Fig. 1) from the centre of the (Pb, Pb, 0) system. The data point fit to a two component exponential attenuation curve of the form given by Eq. (2).

from, Eq. (1)a half-thickness ($L_{1/2}$) can be calculated, where $L_{1/2}$ is defined as the moderator thickness x, that result in reduction of the overall neutron flux by a factor of two. For neutrons of $E_n \leqslant 20$ MeV, half-thickness values are 25 and 18.5 cm for (Pb,Pb,0) and (Pb,C,0) systems, respectively.

From Fig. 5, it can be seen that in the case of the (Pb,Pb,^{235}U) system, the variation of the neutron flux $F(x)$ with x, is very different from the cases of non-multiplying systems and it cannot be described by an exponential attenuation curve.

In Fig. 6 neutron flux as a function of distance, for the (Pb, Pb, 0) system and for $E_n \leqslant 20$ MeV is shown which also includes the flux-values for $x < 15$ cm. When all flux-values with $x \geqslant 0$ cm are included, the results cannot be expressed in terms of a first order exponential attenuation curve (Eq. (1)). However the data points shown in Fig. 6 have a near perfect fit to a two-component exponential attenuation curve of the form:

$$F(x) = y_0 + A_1 e^{-(x-x_0)/t_1} + A_2 e^{-(x-x_0)/t_2}, \quad x \geqslant 0, \quad (2)$$

The parameters of the Eq. (2) for 10^9 incident protons of 2.5 GeV/c are as follows: $y_0 = 0 \pm 0$, $x_0 = 0 \pm 0$ cm,
$A_1 = (60.693 \pm 2.933) \times 10^7$ n cm^{-2}s^{-1},
$t_1 = 3.882 \pm 0.350$ cm,
$A_2 = (109.619 \pm 2.876) \times 10^7$ n cm^{-2}s^{-1} and
$t_2 = 36.381 \pm 1.139$ cm.

In Fig. 6 the best-fit curve to the calculated fluxes as well as the curves describing the two components of the attenuation curve are shown. The first component of the Eq. (2) has an attenuation length of $t_1 = 3.88$ cm and a half-length of $(L_1)_{1/2} = 2.69$ cm. The attenuation-length and half-length of the more penetrating component are identical (within statistical errors) to those obtained from Eq. (1) (Table 1). The first component of the attenuation curve dies away for $x \geqslant 15$ cm.

Detailed analysis of the results showed that the presence of two exponential components in Eq. (2), is not the consequence of the difference in the size of the calculation cells at $x < 15$ and $x \geqslant 15$ cm. We deliberately used larger cell sizes for $x \geqslant 15$ cm to reduce the statistical errors of the calculations.

To understand the behaviour of the attenuation curves in Fig. 6, we calculated the spallation neutron yield Y_n as a function of target radius R, for a lead target of length $L = 100$ cm at incident proton energy of 1.73 GeV (see also Ref. [10]). The radius was varied from 0.5 cm (the beam radius) to 140 cm. In Fig. 7, variations of Y_n and spallation neutron yield per unit radius S_n, ($S_n = \Delta Y_n / \Delta R$)

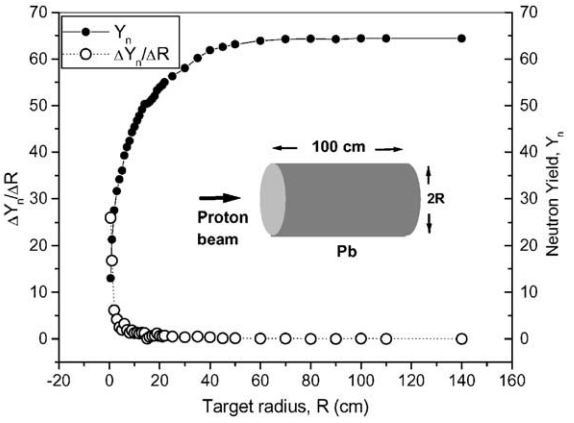

Fig. 7. Variations of Y_n and spallation neutron yield per unit radius S_n, ($S_n = \Delta Y_n/\Delta R$) with the target radius R.

with the R (same as X in Fig. 6) is shown. It can be seen that Y_n approaches to a plateau value and S_n falls almost exponentially with increasing R. This suggests that the attenuation curves shown in Fig. 6 carry information on the spatial distribution of the primary spallation neutrons within the spallation source volume besides the effects of the scattering of the same neutrons in the moderator.

The spallation neutrons are produced by means of intranuclear cascade, evaporation and/or fission and inter-nuclear cascade processes. The latter can take place in all available volume of the target (and moderator if present) as long as the energy requirements of the process are satisfied. However the other reactions mainly occur in the volume that contains the proton beam, which in our case is the interior of a cylindrical volume of radius 0.5 cm. Therefore we believe that the fast decaying curve (Fig. 6) in fact to some extent, describes the decay of the inter-nuclear cascade process with the distance.

Fig. 8a shows the variation of the flux of the low energy neutrons ($E_n \leqslant 1$ eV) with the distance x, for the all three systems studied. As already shown in Figs. 3c and 4 the number of slow neutrons in the case of the graphite moderator is much higher than the other two systems. In (Pb,Pb,0) system the variation of the $F(x)$ with x ($x \geqslant 15$ cm) can be described by a second order polynomial. However this is not the case with (Pb,C,0) and (Pb,Pb,^{235}U) systems. The slow neutron flux in the vicinity of the multiplying region is highly depressed (as expected).

Fig. 8b illustrates the variation of the neutron flux with distance x for neutrons with energy in the range of $1\,\text{eV} < E_n \leqslant 1\,\text{keV}$. Such neutrons are important for nuclear transmutation by adiabatic resonance crossing method [4,5]. As seen in Fig. 8b the neutron multiplying region highly enhances the number of the neutrons that are relevant to TARC. Also from Fig. 8b it is evident that, as for neutrons with $E_n \leqslant 1$ eV (Fig. 8a) the neutron flux within and in the neighbourhood of the multiplying region ($64 < x < 107$ cm) is highly depressed. Therefore in order to exploit the increased neutron flux (because of the presence of a neutron multiplier), one has to avoid the vicinity of the fissile material region. Thus in the case of the (Pb,Pb,^{235}U) system discussed in this paper we are restricted to the volume with $x < 60$ cm (Fig. 8b).

In the case of the (Pb,C,0) system effectively regions with $x < 30$ cm will be useful for transmutation by resonance capture and indeed in this region the neutron flux can compete with (Pb,Pb,^{235}U) system. Note that for the (Pb,C,0) system at x-values of < 30 cm the flux of neutrons relevant to transmutation via resonance capture is higher by a factor of up to two, compared to the (Pb,Pb,0) system.

As already mentioned, not only the flux of the slow neutrons (< 1 eV) but in general the flux of all neutrons of energy less than ~ 1 keV is highly depressed (within and in the neighbourhood of the neutron multiplying region (Figs. 8a and b)). This is expected, and is a common feature of the heterogeneous nuclear systems. Thus in an ADS, using large volume of lead as a neutron moderator-storage medium (for a given k_{eff} -value) one needs to minimise the volume of the neutron multiplying region (the fissile material) to increase the available high-flux volume in the system, for transmutation applications. Therefore if an ADS is designed for nuclear waste transmutation by means of TARC, a heterogeneous lattice structure with fuel elements spread throughout the moderating environment does not seem to be a suitable choice. One will not have such restrictions in

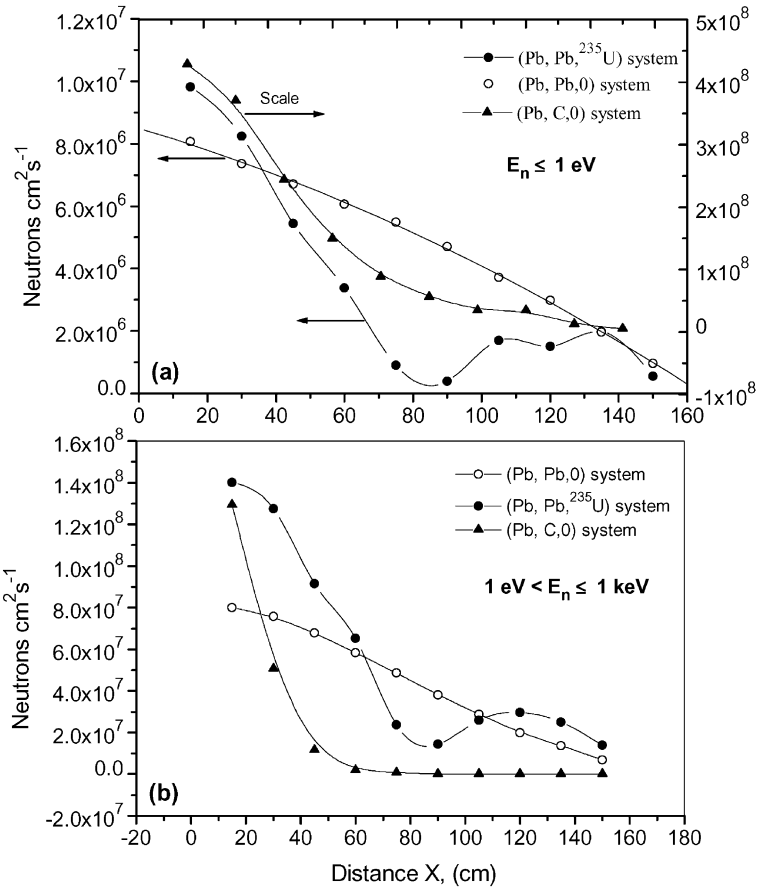

Fig. 8. (a) Flux of neutrons of energy $\leqslant 1$ eV as a function of distance x, from the centre of the assemblies. Distance x, was measured on the X-axis (Fig. 1). (b) Variation of flux of neutrons of energy 1 eV $< E_n \leqslant 1$ keV with of distance, x.

homogenous systems where the fissile and moderating materials are uniformly mixed.

6. Conclusions

We used the LAHET code system to study the behaviour of spallation neutrons resulting from interaction of 2.5 GeV/c protons with a massive lead target within large ($3.3 \times 3.3 \times 3\,m^3$) lead and graphite moderating environments.

It is shown that with lead moderator the peak of the energy distribution of neutrons appears at ~ 520 keV in the presence or absence of a neutron-multiplying medium in the system. This is independent of the location within the moderator.

In the case of the graphite moderator as expected the neutron field is dominated by slow neutrons ($E_n < 1$ eV) while in the lead moderator the slow neutron flux does not exceed 8.4% of the total neutron flux at a given location.

The variation of the neutron flux ($E_n \leqslant 20$ MeV) with distance x (Fig. 1), for both lead and graphite moderators (in the absence of any fissile material in the system) can be described very well using a first order exponential attenuation curve for $x \geqslant 15$ cm. We obtained attenuation length of 36 and 26.7 cm for lead and graphite moderators, respectively. In the case of the lead moderator when the flux values corresponding to $x < 15$ cm are included in the plots, a two component exponential attenuation curve gives an excellent

fit to the data. We believe that the fast decaying component of the attenuation curve to some extent describes the decay of the inter-nuclear cascade process with the distance from the centre of cascade.

The observed differences in the energy spectra of the neutrons in graphite and lead moderators are expected to result in noticeable differences in the transmutation abilities of the (Pb,Pb,0) and (Pb,C,0) systems, under the same operational conditions [13].

Acknowledgements

SRH-N wishes to thank Prof. L.S. Peak and Dr. J. Ulrichs for comments and suggestions. An Institutional Grant of the Australian Research Council (ARC) supported this research program.

References

[1] C.D. Bowman, et al., Nucl. Instr. and Meth. A 320 (1992) 336.
[2] C. Rubbia, et al, Conceptual design of a fast neutron operated high power energy amplifier, CERN/AT-95-44, 1995.
[3] J.-S. Wan, et al., Kerntechnik 63 (1998) 167.
[4] C. Rubbia, Resonance enhanced neutron captures for element activation and waste transmutation. CERN/LHC/97-04, 1997.
[5] H. Arnould, et al., Phys. Lett. B 458 (1999) 167.
[6] Charles D. Bowman, Sustained Nuclear Energy Without Weapons or Reprocessing using Accelerator-Driven Systems, in: M. Hron, V. Lelek, M. Mikisek, M. Sinor, J. Uher, J. Zeman (Eds.), Proceedings of the Third International Conference on Accelerator Driven Transmutation Technologies and Applications, Parha, Czech Republic, June 7–11, 1999.
[7] The joint project for high-intensity proton accelerators, KEK Report 99-4, JAERI-Tech 99-056, JHF-99-3, July 1999, p. 37–46.
[8] Richard E. Prael and Henry Lichtenstein, User guide to LCS: the LAHET code system, Los Alamos National Laboratory, Report LA-UR-89-3014, September 1989.
[9] Judith F. Briesmeister (Ed.), MCNP-4B—A general Monte Carlo *N*-particle transport code, Los Alamos National laboratory, Report LA-12625-M, March 1997.
[10] S.R. Hashemi-Nezhad, et al., Kerntechnik 66 (2001) 47.
[11] S.R. Hashemi-Nezhad, et al., Monte Carlo studies of accelerator driven systems: energy and spatial distribution of neutrons in multiplying and non-multiplying media, JINR Report E1-2000-291, 2000.
[12] J.R. Lamarsh, Introduction to Nuclear Reactor Theory, Addison-Wesley Publishing Company Inc., Reading, MA, 1966.
[13] S.R. Hashemi-Nezhad, et al., Monte Carlo calculations on transmutation of transuranic nuclear waste isotopes using spallation neutrons: difference of lead and graphite moderators, JINR Report E1-2001-44, 2001, Nucl. Instr. and Meth. A 481 (2002), this issue.